![Texas Instruments logo]

Respiration Rate Measurement Based on Impedance Pneumography

Amit K. Gupta   *Data Acquisition Products*

ABSTRACT

This document discusses the use of impedance pneumography as a technique to measure respiration rate. The generation of high-frequency ac current source is described, and the issues related to delay in modulated signal and finite transition times of carriers are addressed. The report also includes descriptions of potential implementations of a respiration rate measurement system using the ADS1298R and the respective respirative impedance measurement results.

Contents

List of Figures

All trademarks are the property of their respective owners.

1 Introduction

Impedance pneumography is a commonly-used technique to monitor a person's respiration rate, or breathing rate. It is implemented by either using two electrodes (Figure 1**a**) or four electrodes (Figure 1**b**). The objective of this technique is to measure changes in the electrical impedance of the person's thorax caused by respiration or breathing.
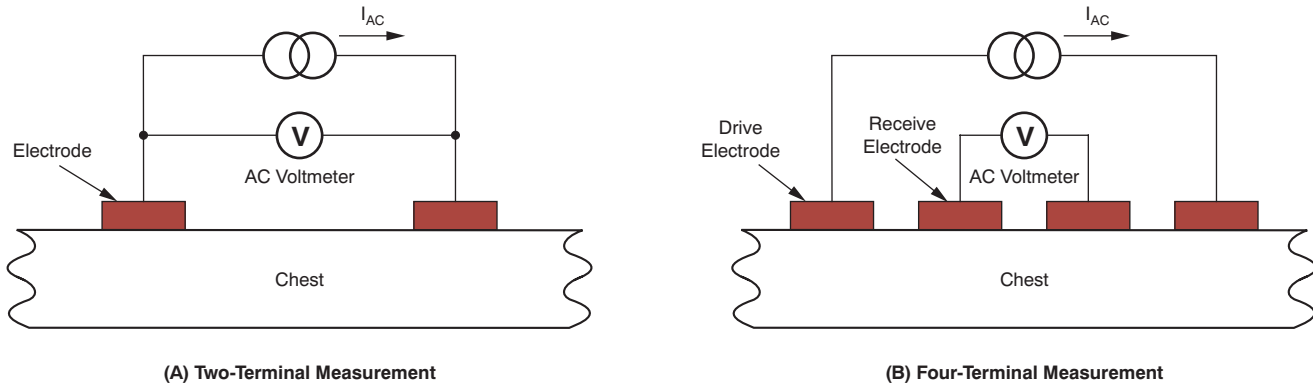

Figure 1. Arrangement of Electrodes for Impedance Pneumography

In both of these methods, a high-frequency ac current is injected into the tissue through the drive electrodes (see Ref. 1). The ac current causes a potential difference to develop across any two points between the drive electrodes. This potential difference is related to the resistivity of the tissue between the voltage-sensing or *receive* electrodes. The equivalent resistance is defined as the ratio of the voltage difference between the two receive electrodes and the current that flows through the tissue.

The two-terminal measurement configuration (shown in Figure 1**a**) introduces some errors because the potential difference sensed between the two electrodes includes the nonlinear voltages generated by the current flowing through the polarization impedance at the electrode-tissue interface. The four electrode configuration, illustrated in Figure 1**b**, yields a more precise measurement because the sites of current injection and voltage measurement are physically separated, but require two additional electrodes. Therefore, the two-electrode measurement shown in Figure 1**a** is the most commonly used; the normal electrocardiogram (ECG) electrodes can be used for respiration as well.

2 Thoracic Impedance Model

When measuring respiration, the thorax presents an electrical impedance to the electrode that consists of two impedance components: a relatively constant value and a varying value. The relatively constant value of thoracic impedance is referred to in this document as the *baseline impedance*, or R_B (typically 500 Ω; see Ref. 2). The varying value, on the other hand, is known as *respirative impedance*, or ΔR. Changes in the electrical resistance of the lungs are mainly a result of the following two effects:

1. During inspiration, there is an increase in the gas volume of the chest in relation to the fluid volume; this increase causes conductivity to decrease.
2. During inspiration, the length of the conductance paths increases because of expansion.

Taken together, both of these effects cause the electrical impedance to increase (see Ref. 3). There is a good correlation between this impedance change and the volume of respirated air. This relationship is approximately linear. The varying component of impedance (that is, respirative impedance), generates a varying voltage component (ΔV) when current is injected. This varying voltage component is the parameter of interest because this component can then be used to determine the person's breathing rate. Typically, ΔR is in the range of 0.1 Ω to 1 Ω. ΔV, in turn, depends on the magnitude of the current injected.

Figure 2 presents an electrical model of the respiration circuit. This model includes the defibrillator protection resistances (R_P) in each wire of the ECG cable (about 1 kΩ per wire) and the electrode impedance ($Z_{Electrode}$). The electrode impedance is modeled as a 51-kΩ resistor in parallel with a 47-nF capacitor as specified in the ANSI/AAMI EC13:2002 standard. The total baseline impedance (R_{Beff}) consists of the sum of R_P, R_B, and $Z_{Electrode}$.
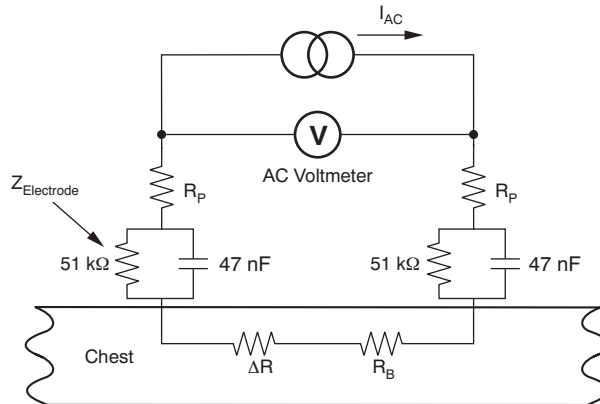

Figure 2. Respiration Circuit Electrical Model

3   Amplitude Modulation/Demodulation

As explained earlier, impedance pneumography requires injecting current into the body. The ANSI/AAMI ES1-1993 standard allows injecting up to 100 µA of current at 10 kHz. At lower frequencies, of course, the current that can be injected into the body is lower.

For respiration, a high-frequency ac signal is injected into the body; this signal acts as a carrier that is amplitude-modulated by the low-frequency signal (ΔV) generated as a result of the breathing action. On the receiver side, this modulated signal must be demodulated in order to extract the low-frequency breathing signal. After demodulation, the signal is low-pass filtered to the 2-Hz to 4-Hz bandwidth level to remove unwanted noise. The demodulated and filtered output, generally, is then digitized by a high-precision analog-to-digital converter (ADC).

Figure 3 shows the entire signal chain concept in a block diagram. The carrier at frequency F_C can be either sine wave or square wave. The demodulation is accomplished with a square wave signal at the same frequency. Capacitor C_T blocks any dc current from reaching the body on the transmission side, while capacitor C_R is used for the same purpose on the receiver side. Ideally, we prefer to keep this capacitance as small as possible so that at line frequencies (50 Hz to 60 Hz), any impedances looking from the body to both the transmitter and receiver sides are high. In practice, however, the capacitors are chosen to be large enough so that the carrier is not significantly attenuated.
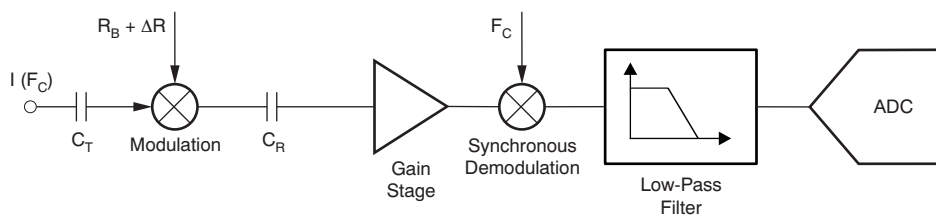

Figure 3. Conceptual Block Diagram of the Signal Chain

3.1 The Carrier Signal

The carrier signal is often generated in the voltage domain, and converted to a current by passing through a resistor. The configuration shown in Figure 4(a) produces only a pseudo-constant current because it varies with changes in R_{Beff} and ΔR. As mentioned earlier, the baseline impedance (R_{Beff}) consists of the cable resistance and the electrode impedance, and the fixed impedance of the thoracic cavity. Figure 4(b) shows the generation of a square wave modulation signal. In the first half cycle, node X is connected to V_A and node Y to V_B (a solid line connection). In the second half cycle, the connection is reversed, with node X connected to V_B and node Y to V_A (a dotted line connection). This configuration generates a square wave at node X and Y at the frequency of toggling (that is, F_C). Both signals V_A and V_B must be low noise.

$$I_{AC} \approx \frac{V}{2 \cdot R_T + R_{Beff}}$$

$$I_{ACpp} \approx \frac{2 \cdot (V_A - V_B)}{2 \cdot R_T + R_{Beff}}$$

(a) General Concept   **(b) Square Wave Carrier Implementation**
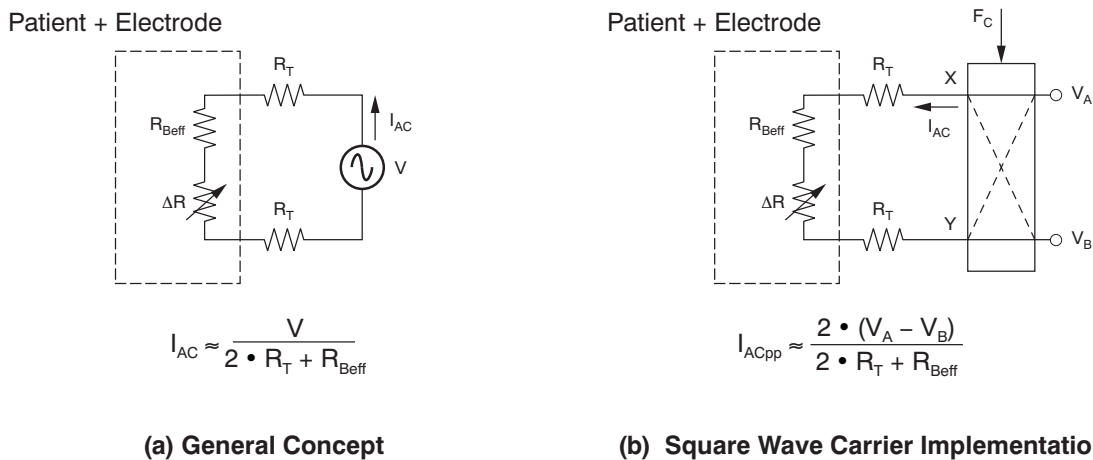
Figure 4. Generating the Carrier Current

The sine wave carriers are much more difficult to generate. One possible solution is to use the direct digital synthesis (DDS) technique. DDS is a method of producing an analog waveform by generating a time-varying signal in digital form and then performing a digital-to-analog conversion. In certain cases, a square wave may be heavily filtered to created carrier signals that look similar to a sine wave.

3.2 Square Wave Carrier Demodulation

The demodulation signal is simply a square wave signal at the same frequency as the modulation signal. The phase of the demodulation signal must be adjusted to account for the phase delay in the signal path. If the phase is not adjusted properly, the demodulator gain drops. Figure 5 illustrates the effect of time delay on the demodulator output for square wave modulation. Here, the modulated signal is delayed by t_D before it reaches the demodulator. If the demodulator clock has the same phase as the modulation clock [as shown in Figure 5(a)], the gain of the demodulator is not unity.
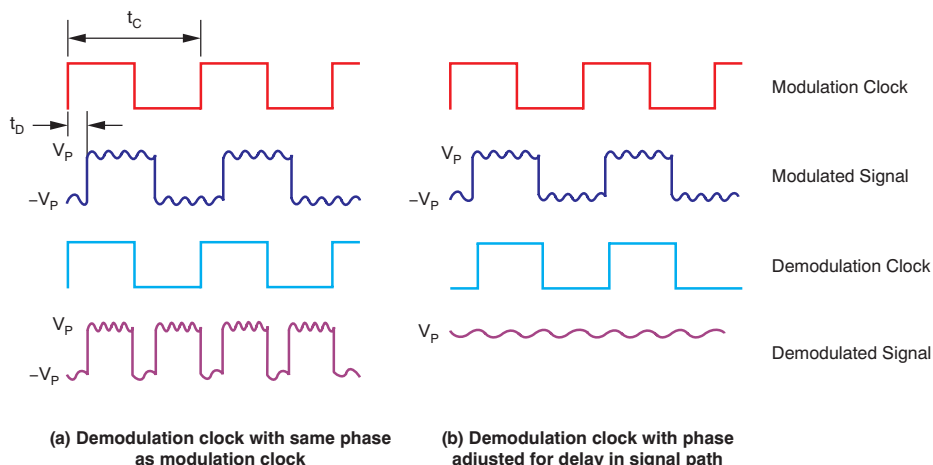

(a) Demodulation clock with same phase as modulation clock   **(b) Demodulation clock with phase adjusted for delay in signal path**

Figure 5. Effect of Delay in Signal Path

The demodulator gain with a delay is calculated as $\dfrac{(t_C - 4t_D)}{t_C}$ which drops to 0 if $t_D = \dfrac{t_C}{4}$.

Figure 5(b) illustrates how phase shifting the demodulation clock can bring the demodulator gain back to unity. The carrier signal is low-pass filtered because of cable capacitance and also as a result of the finite bandwidth of the front-end amplifiers. This filtering leads to slow rise and fall times on the modulated signal, which then must be demodulated. In this case, we can phase-shift the demodulator clock to account for the delay, but finite rise/fall times can continue to cause the demodulator gain to drop.

Figure 6 illustrates the effect of finite transition times on the demodulated output. The demodulation clock is phase-shifted to account for the delay in the modulated signal. The negative-going glitch on the output causes the gain to drop from unity to about 0.8. The actual drop in gain depends on the fraction of time that the signal spends in transition from low to high and vice-versa.
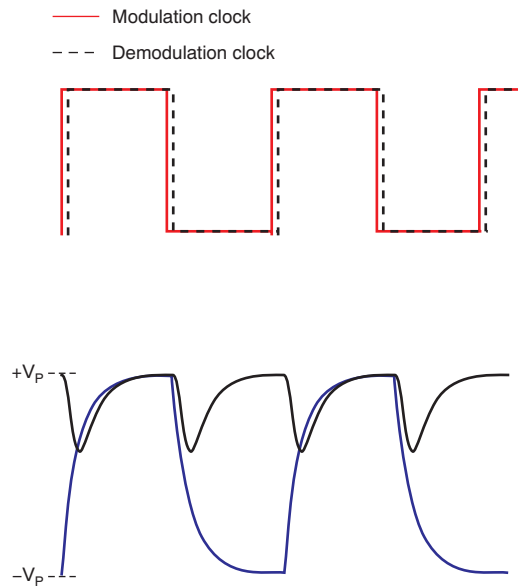

Figure 6. Effect of Finite Transition Time of Modulated Signal

3.3   Sine Wave Carrier Demodulation

For sine wave carriers, the demodulation signal is again a square wave signal at the same frequency as the modulation signal. The phase of the demodulation clock is important because the synchronous demodulator (when properly timed with the zero signal crossings it detects) accomplishes a precision full-wave rectification. Mismatches of the modulated signal zero crossings, relative to the transitions of the demodulation clock, reduce the demodulator gain. For sine wave input signals, the gain is proportional to the cosine of the phase difference between the input signal and the demodulation clock. Figure 7(a) illustrates the demodulation of the sine wave carrier with the demodulation clock properly aligned to incoming signal, whereas Figure 7(b) shows the output for a 45° phase shift between the two signals. The demodulator gain drops to zero if the phase shift between the two signals reaches 90°.
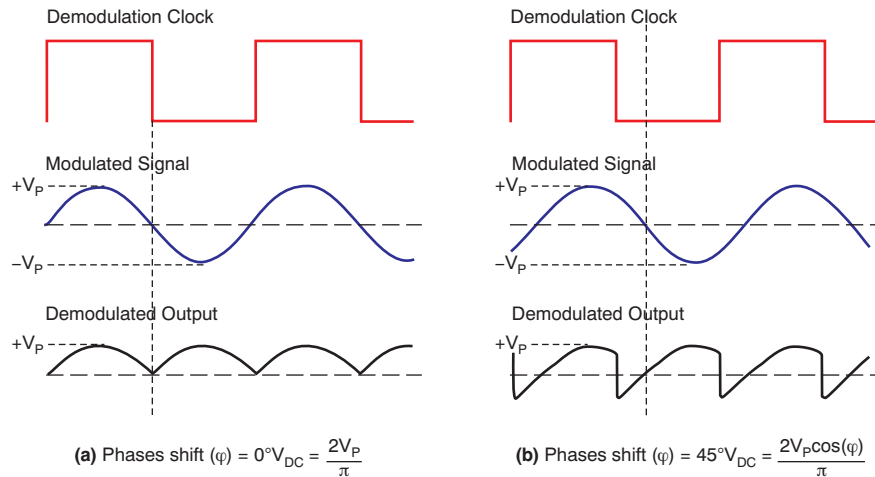
Demodulation Clock

Demodulation Clock

Modulated Signal

Modulated Signal

$+V_P$

$+V_P$

$-V_P$

$-V_P$

Demodulated Output

Demodulated Output

$+V_P$

$+V_P$

(a) Phases shift $(\varphi) = 0° V_{DC} = \dfrac{2V_P}{\pi}$ **(b)** Phases shift $(\varphi) = 45° V_{DC} = \dfrac{2V_P \cos(\varphi)}{\pi}$

Figure 7. Effect of Phase Delay on Demodulation

3.4   Demodulation with Blocking

As discussed in Section 3.1, there are two problems with demodulating a square wave:

- It is difficult to exactly phase-align the modulated signal with the demodulation clock;
- Even if the modulated signal and demodulation clock are phase-aligned, the gain of the demodulator is less than unity because of finite transition times.

To solve these problems, a scheme of demodulation with blocking is illustrated in Figure 8. Here, the gain stage and low-pass filter (LPF) are not continuously connected. When the output of the gain stage (node X) is transitioning, it is disconnected from the input of the LPF (node Y). During the blocking time, node Y holds the previous value. When the transition is complete, the block is removed and the demodulated output is applied to the LPF input. The key requirement for this configuration to work properly is that node Y must be able to retain its previous voltage during the blocking period.
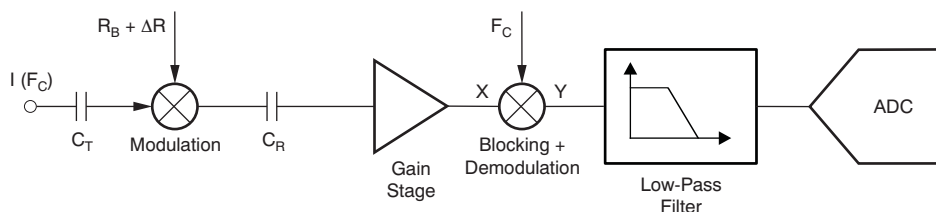
$R_B + \Delta R$

F_C

$I (F_C)$

C_T Modulation C_R Gain Stage   X Blocking + Demodulation Y   Low-Pass Filter   ADC

Figure 8. Signal Chain for Demodulation with Blocking

Figure 9(a) illustrates the demodulation with blocking for 45°, whereas in Figure 9(b) blocking is completed for 90°. The modulated signal in the first case continues to transition when the block is removed, so a negative glitch remains on the output and reduces the gain to about 0.95 compared to the ideal unity gain. In the second case, node X has almost reached its steady state value when the block is removed, so the gain error is less than 1%. The output gain error depends on how much settling error remains at the moment the block is removed. If node Y is high impedance, blocking for a longer period in general results in less gain error.
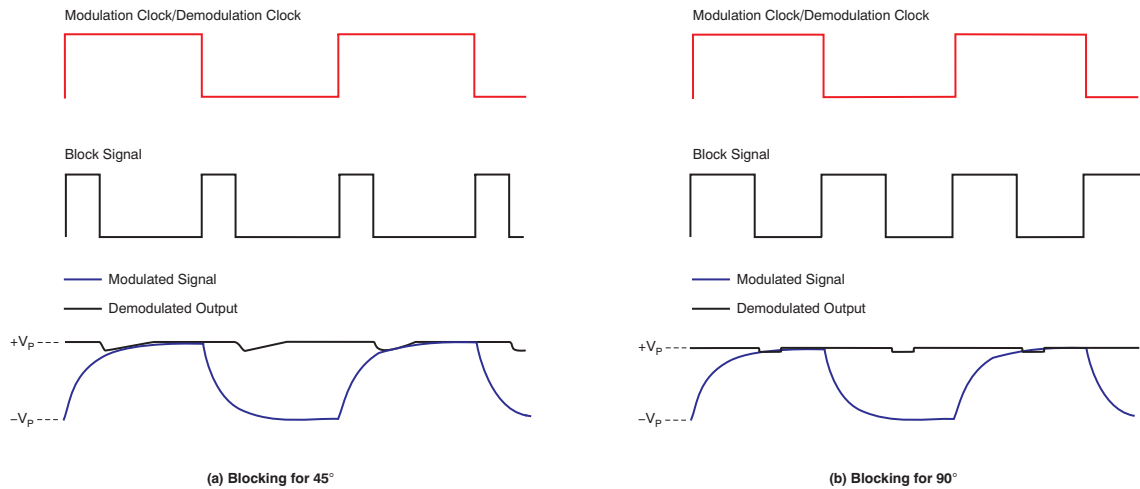

(a) Blocking for 45°   (b) Blocking for 90°

Figure 9. Square Wave Demodulation with Blocking

Figure 10 shows demodulation with blocking for sine wave carriers. Here, the carrier is phase-shifted by 45° with respect to the demodulation clock. If the modulated signal is blocked for 45°, as shown in Figure 10(a), the dc output is approximately 13% higher than the signal shown with precision full-wave rectification in Figure 7(a). If the modulated signal is blocked for 90° as shown in Figure 10(b), only the peak of the signal is captured, and gives approximately a 26% higher dc output than synchronous rectification.
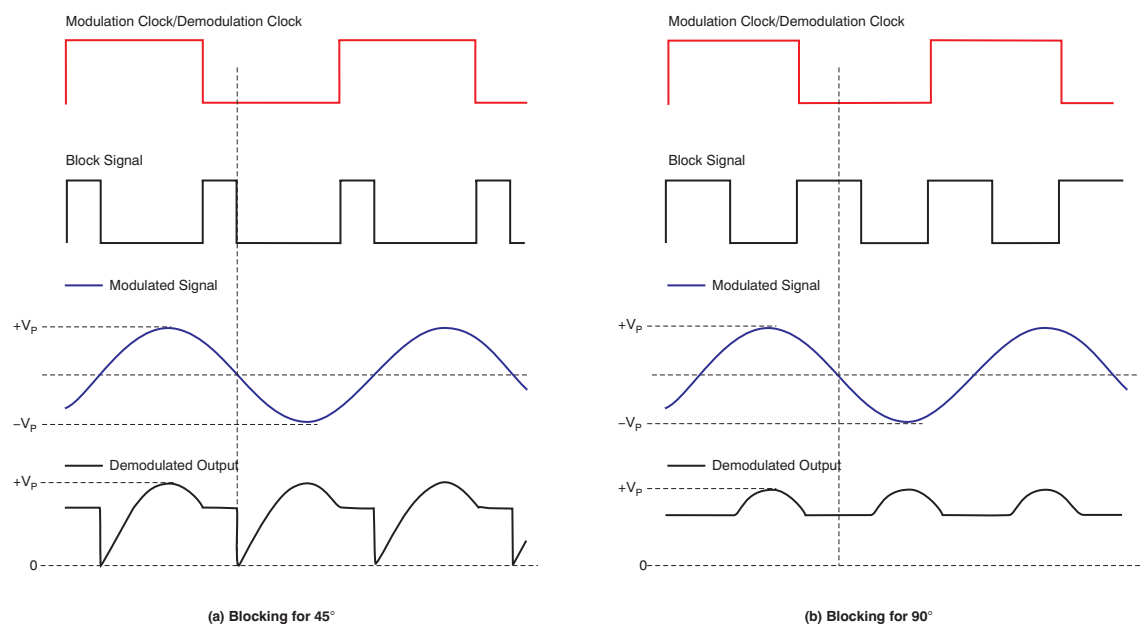

(a) Blocking for 45°   (b) Blocking for 90°

Figure 10. Sine Wave Demodulation with Blocking

The blocking method with sine waves works reasonably well until a phase shift of 135° occurs. If the signal is blocked for the amount of phase shift, the demodulated output is at least equal to the output obtained with full wave rectification. For phase shifts greater than 135°, there is a likelihood of capturing the zero crossing of the signal when the block is removed. Therefore, it is better to not block the signal. It is also important to realize that with a 180° phase shift, the signal and demodulation clock are still perfectly phase-aligned. The polarity of the demodulated output is reversed, which is generally not a concern. For sine wave carriers, then, blocking should not be used for phase shifts greater than 135°.

4 Non-Ideal Effects Because of Cable Capacitance

The cable capacitance, in conjunction with the base impedance, creates a low-pass filter. This filter attenuates the modulated signal. For the increased baseline impedance, the attenuation is larger. This increased attenuation affects the measured respirative impedance (ΔR). For the same ΔR, the measured ΔV is smaller for larger baseline impedances. Therefore, optimization of the square wave carrier would be necessary based on the user's system.

5 Respiration Rate Measurement with ADS1298REVM

The ADS1298R-EVM demonstrates the measurement of respiration rates based on the principle of impedance pneumography, using the ADS1298R. The ADS1298R uses a square wave for modulation. The modulation frequency used is 32 kHz and the on-chip reference is used as the modulating signal. Demodulation is done with the blocking scheme explained earlier. Refer to the ADS1298R-EVM user guide for additional details on using the EVM. A simplified diagram that illustrates the respiration portion of the circuit is shown in Figure 11.
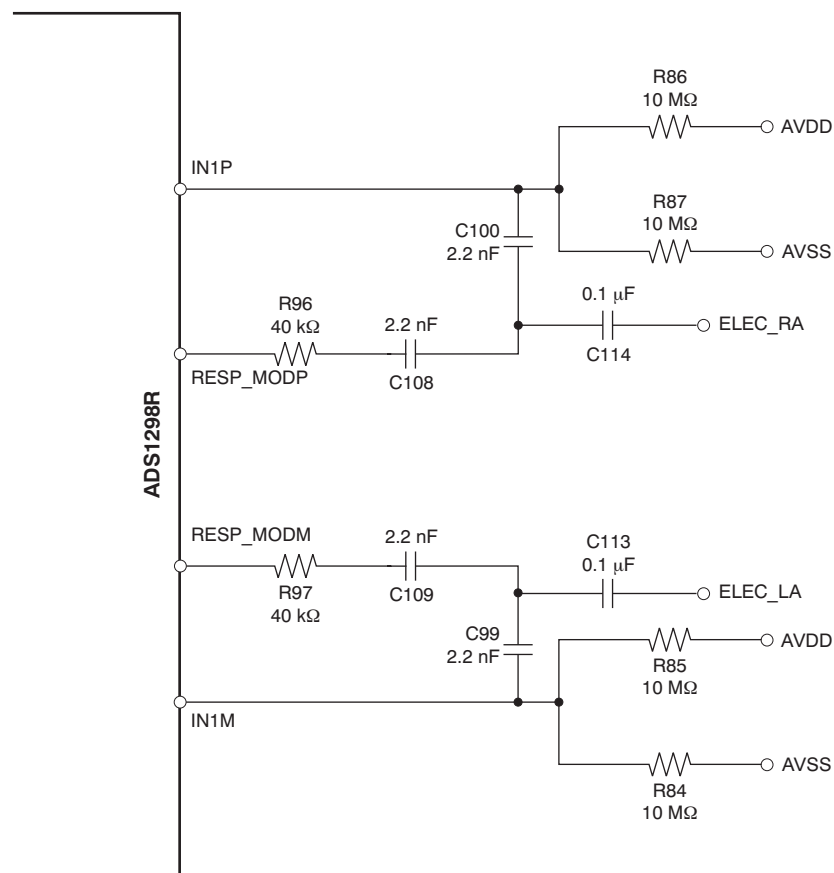

Figure 11. ADS1298R-EVM Respiration Circuitry

In Figure 11, a patient simulator can be connected between leads ELEC_RA and ELEC_LA to provide the baseline impedance (R_B) and the varying component (ΔR). Resistors R96 and R97 limit the amount of ac current that flows into the body. Capacitors C108 and C109 block any dc current from flowing into the body from the transmission side. Capacitors C99 and C100 serve the same purpose on the receiver side. Capacitors C113 and C114 serve as a secondary means to prevent a single fault (for example, a shorted C109 capacitor from a carrier generator) from causing excessive dc currents through the patient. The respiration signals are routed to Channel 1, which has respiration capability.

5.1   Measurement Results

The output from any typical patient simulator with a respiration feature can be directly fed to the ADS1298R-EVM. The results presented here are taken with a Fluke MedSim 300B simulator. This simulator has several options to choose a different base impedance (R_B) and delta impedance (ΔR) on the simulator. For illustration purposes, R_B of 500 Ω is chosen. Figure 12 shows the results with R_B = 500 Ω and ΔR = 1 Ω. Figure 13 shows the results with R_B = 500 Ω and ΔR = 0.1 Ω. This output can be further filtered to the respiration bandwidth to get a clean respiration signal, from which the respiration rate can be calculated.
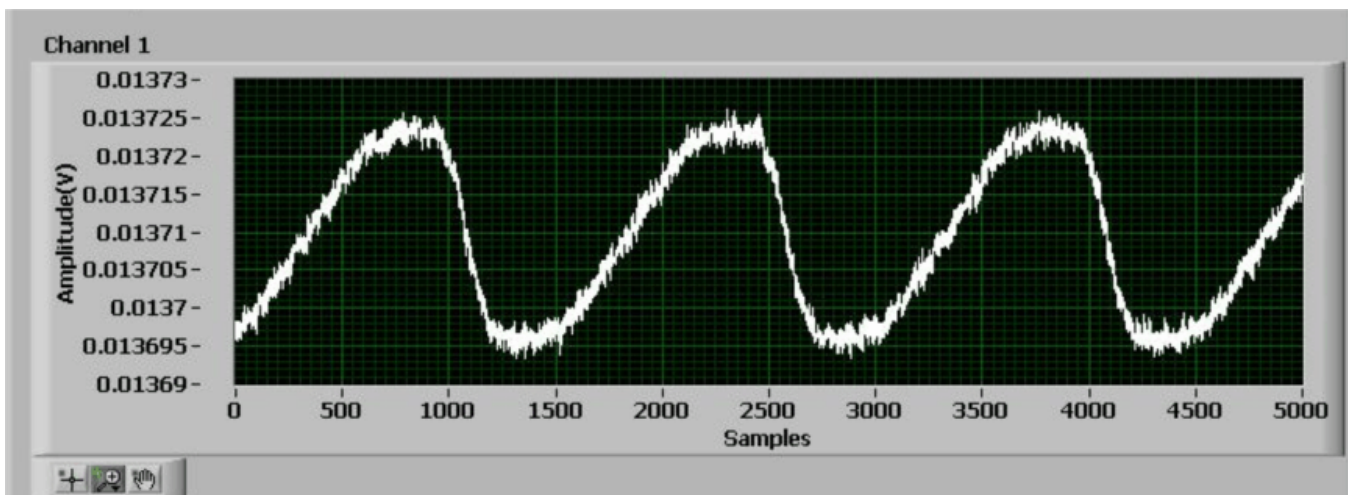

Figure 12. Channel 1 Result for R_B= 500 Ω with Patient Simulator
ΔR = 1 Ω, R_B = 500 Ω, Expected DC = 14.9 mV, Expected ΔV = 29.1 µV
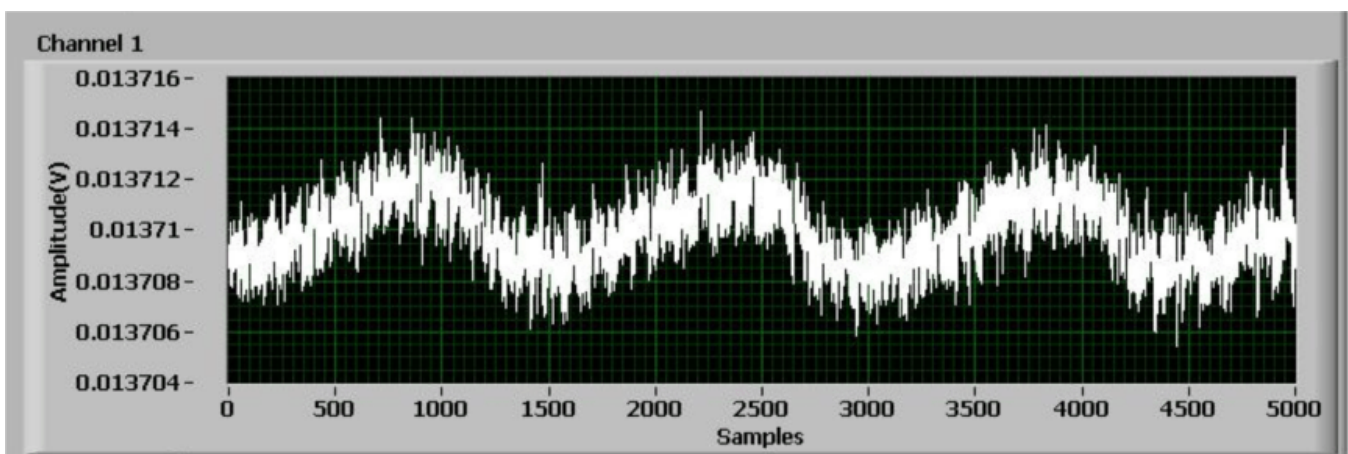

Figure 13. Channel 1 Result for R_B= 500 Ω with Patient Simulator
ΔR = 0.1 Ω, R_B = 500 Ω, Expected DC = 14.9 mV, Expected ΔV = 2.91 µV

The expected dc output can be calculated as shown in Equation 1:

$$DC\_V = \frac{R_B}{R_B + R96 + R97} \cdot (VREFP - VREFM)$$

$$= \frac{0.5\ k}{0.5\ k + 40\ k + 40\ k} \cdot 2.4 = 14.9\ mV$$

(1)

Current flowing through the body, or I_B, is calculated according to Equation 2:

$$I_B = \frac{VREFP - VREFM}{R96 + R97 + R_B} = \frac{2.4}{80.5\ k} = 29.81\ \mu A$$

(2)

The peak-to-peak output can be calculated as Equation 3.

$$\Delta V = \Delta R \cdot I_B = 1 \cdot 29.15 = 29.1\ \mu V \qquad (\Delta R = 1\ \Omega)$$

$$\Delta V = \Delta R \cdot I_B = 0.1 \cdot 29.15 = 2.91\ \mu V \qquad (\Delta R = 0.1\ \Omega)$$

(3)

6 References

1. Prutchi, D. and M. Norris. (2004). Design and development of medical electronic instrumentation: A practical perspective of the design, construction, and test of medical devices. Hoboken, NJ: Wiley Interscience.
2. Grenvik, A., Ballou, S., McGinly, E., Cooley, W.L., and P. Safar. (1972). Impedance pneumography: Comparison between chest impedance changes and respiratory volumes in 11 healthy volunteers. *Chest*, vol 62, pp. 439-443.
3. Kelkar, S.P., Khambete, N.D., and S.S. Agashe. (2008). Development of movement artefacts free breathing monitor. *Journal of the Instrument Society of India*, vol. 38, pp. 34-43.

IMPORTANT NOTICE

Texas Instruments Incorporated and its subsidiaries (TI) reserve the right to make corrections, modifications, enhancements, improvements, and other changes to its products and services at any time and to discontinue any product or service without notice. Customers should obtain the latest relevant information before placing orders and should verify that such information is current and complete. All products are sold subject to TI's terms and conditions of sale supplied at the time of order acknowledgment.

TI warrants performance of its hardware products to the specifications applicable at the time of sale in accordance with TI's standard warranty. Testing and other quality control techniques are used to the extent TI deems necessary to support this warranty. Except where mandated by government requirements, testing of all parameters of each product is not necessarily performed.

TI assumes no liability for applications assistance or customer product design. Customers are responsible for their products and applications using TI components. To minimize the risks associated with customer products and applications, customers should provide adequate design and operating safeguards.

TI does not warrant or represent that any license, either express or implied, is granted under any TI patent right, copyright, mask work right, or other TI intellectual property right relating to any combination, machine, or process in which TI products or services are used. Information published by TI regarding third-party products or services does not constitute a license from TI to use such products or services or a warranty or endorsement thereof. Use of such information may require a license from a third party under the patents or other intellectual property of the third party, or a license from TI under the patents or other intellectual property of TI.

Reproduction of TI information in TI data books or data sheets is permissible only if reproduction is without alteration and is accompanied by all associated warranties, conditions, limitations, and notices. Reproduction of this information with alteration is an unfair and deceptive business practice. TI is not responsible or liable for such altered documentation. Information of third parties may be subject to additional restrictions.

Resale of TI products or services with statements different from or beyond the parameters stated by TI for that product or service voids all express and any implied warranties for the associated TI product or service and is an unfair and deceptive business practice. TI is not responsible or liable for any such statements.

TI products are not authorized for use in safety-critical applications (such as life support) where a failure of the TI product would reasonably be expected to cause severe personal injury or death, unless officers of the parties have executed an agreement specifically governing such use. Buyers represent that they have all necessary expertise in the safety and regulatory ramifications of their applications, and acknowledge and agree that they are solely responsible for all legal, regulatory and safety-related requirements concerning their products and any use of TI products in such safety-critical applications, notwithstanding any applications-related information or support that may be provided by TI. Further, Buyers must fully indemnify TI and its representatives against any damages arising out of the use of TI products in such safety-critical applications.

TI products are neither designed nor intended for use in military/aerospace applications or environments unless the TI products are specifically designated by TI as military-grade or "enhanced plastic." Only products designated by TI as military-grade meet military specifications. Buyers acknowledge and agree that any such use of TI products which TI has not designated as military-grade is solely at the Buyer's risk, and that they are solely responsible for compliance with all legal and regulatory requirements in connection with such use.

TI products are neither designed nor intended for use in automotive applications or environments unless the specific TI products are designated by TI as compliant with ISO/TS 16949 requirements. Buyers acknowledge and agree that, if they use any non-designated products in automotive applications, TI will not be responsible for any failure to meet such requirements.

Following are URLs where you can obtain information on other Texas Instruments products and application solutions:

Products		Applications	
Audio	www.ti.com/audio	Communications and Telecom	www.ti.com/communications
Amplifiers	amplifier.ti.com	Computers and Peripherals	www.ti.com/computers
Data Converters	dataconverter.ti.com	Consumer Electronics	www.ti.com/consumer-apps
DLP® Products	www.dlp.com	Energy and Lighting	www.ti.com/energy
DSP	dsp.ti.com	Industrial	www.ti.com/industrial
Clocks and Timers	www.ti.com/clocks	Medical	www.ti.com/medical
Interface	interface.ti.com	Security	www.ti.com/security
Logic	logic.ti.com	Space, Avionics and Defense	www.ti.com/space-avionics-defense
Power Mgmt	power.ti.com	Transportation and Automotive	www.ti.com/automotive
Microcontrollers	microcontroller.ti.com	Video and Imaging	www.ti.com/video
RFID	www.ti-rfid.com	Wireless	www.ti.com/wireless-apps
RF/IF and ZigBee® Solutions	www.ti.com/lprf		

TI E2E Community Home Page   e2e.ti.com